Frequency−Time-Resolved Four-Wave Mixing of a Dye Molecule in Liquid

Sang-Hoon Lee, June-Sik Park, and Taiha Joo*

Division of Molecular and Life Science, Department of Chemistry, Pohang University of Science and Technology (POSTECH), Pohang, 790-784, Korea

Received: February 17, 2000; In Final Form: June 1, 2000

Time-resolved ground-state bleach and excited-state stimulated emission spectra are measured for a cyanine dye, 3,3′-diethylthiatricarbocyanine iodide, dissolved in methanol by spectrally resolving a background-free three pulse four-wave mixing signal. It has been shown from model theoretical calculations and experiments that dynamics of the nuclear wave packets created in both ground and excited electronic states can be observed through the oscillations of the spectral line width as well as the center frequency in time. For a system with small Stokes shift, where the ground-state bleach and the stimulated emission spectra cannot be resolved into two separate bands, unambiguous assignment of an oscillation in the whole spectra to either the ground or the excited electronic state could be made by comparison between the phase of the oscillation in center frequency and that in line width.

1. Introduction

Femtosecond spectroscopy is one of the most powerful and widely used tools for the study of ultrafast chemical and physical processes in condensed phases. One exciting feature of the femtosecond spectroscopy is its capability to observe and to control nuclear motions in real time by the formation of nuclear wave packets (coherent superposition of the vibrational wave functions).[1] In fact, oscillations of a signal trace in time due to nuclear wave packet motions are ubiquitous in femtosecond spectroscopies such as transient absorption (TA), time-resolved fluorescence,[2,3] and photon echoes.[4−6] When time-dependent transition frequencies between two electronic states are measured, direct mapping between energy difference of the electronic states and a nuclear coordinate may be obtained from a wave packet motion along the potential surface.[7,8] In an ideal case, detailed molecular dynamics of an elementary chemical reaction can be studied by observing the nuclear wave packet motion along the reaction coordinate.

In a typical femtosecond spectroscopic measurement, signal is time-integrated at a single wavelength and time resolution is achieved by varying time delays between input pulses. However, conclusions drawn from a time integrated signal at a single frequency are often misleading due to the complicated spectral dynamics caused by solvation dynamics, excited-state absorption, and other physical and chemical processes. A full set of frequency- and time-resolved data is usually necessary to extract a clear picture for the dynamics of a system. For example, in typical resonant third-order nonlinear spectroscopies such as pump/probe TA, an oscillation observed in time trace is due to a nuclear wave packet motion created in either the ground or the excited electronic states. Assignment of the vibration to either electronic state cannot be made, unless a special detection scheme is employed such as probing to a higher electronic state or using tailored femtosecond pulses.[9] The assignment can also be made unambiguously, in favorable cases, by performing TA measurements at several different wavelengths, since the excited-state stimulated emission and the ground-state bleach signals appear at different frequencies. That is, frequency−time-resolved data may allow wave packet dynamics in the ground and the excited electronic states to be observed separately.

Femtosecond time-resolved spontaneous emission measurement by sum frequency generation (SFG) between the spontaneous emission and a gate pulse is a powerful technique to obtain time-resolved spectra,[10,11] in which excited-state dynamics are recorded exclusively. The majority of the time domain data on solvation dynamics have been acquired by this technique.[12−14] Obtaining a full spectrum by SFG, however, is both time-consuming and limited in time resolution to ∼100 fs due to experimental difficulties and inherent frequency−time uncertainty in the SFG. Time-resolved spectra can also be obtained by spectrally resolving probe pulses in a pump/probe TA.[15] The time resolution is solely determined by the duration of the pulses. Recent advances in pump super-continuum probe TA enable the recording of full transient spectra with sub 100 fs time resolution.[16] Photoisomerization of a dye molecule[17] and solvation dynamics[18] have been studied with 40 fs time resolution by this technique.

In pump/probe TA, the third-order signal polarization is generated into a probe pulse wave vector direction. The signal is naturally heterodyned with the probe pulse, and phase sensitive detection greatly increases the measurement sensitivity. In a typical TA spectra measurement, however, an array detector is usually employed to measure the intensity spectra of the probe pulses with and without pump pulses. An alternative to TA is to use two separate pump pulses to generate a third-order signal into a background free direction and spectrally resolve the signal subsequently, i.e., spectrally resolved transient grating (TG) measurements.[19] The time resolution is solely determined by the duration of the input pulses. The background free detection may be advantageous over the differential measurement as in TA in terms of the signal-to-noise ratio, because probe pulses usually have much higher intensity than the signal. In addition, the three-pulse scheme provides the possibility of controlling the states of matter by controlling the time delay between the two pump pulses.[20]

* Corresponding author. Fax: +82-54-279-3399; e-mail: thjoo@postech.ac.kr.

10.1021/jp000631f CCC: $19.00
Published on Web 07/11/2000

In this paper, we report sub 20 fs time-resolved transient spectra measurements by spectrally resolved four-wave mixing (SRFWM) of a cyanine dye, 3,3′-diethylthiatricarbocyanine iodide (DTTCI), dissolved in methanol. Feasibility of obtaining high-quality frequency−time-resolved data with good time resolution by SRFWM is demonstrated. In the analysis, we focus on the observation of the nuclear wave packet dynamics in both the ground and the excited electronic states through the time evolution of the full spectra.

2. Theoretical Background

The experimental arrangement employed in this study is shown in Figure 1. Double-sided Feynman diagrams to generate the third-order polarization are also shown. Two pump pulses k_1 and k_2, separated by a time delay τ, excite the sample to create a transient grating. A third probe pulse k_3, delayed by T from k_2, is diffracted off the transient grating into a background-free $-k_1 + k_2 + k_3$ phase matching direction. The diffracted signal is spectrally dispersed and recorded by an array detector to give a frequency−time-resolved spectrogram, $I(\omega;\tau,T)$. The time delays τ and T correspond to electronic coherence and population periods, respectively, in the time evolution of a system density matrix. Although k_1 and k_2 are overlapped in time in the present experiment, consideration of the effect of finite pulse duration requires the inclusion of τ.

The SRFWM signal can be written as a modulus squared of a Fourier transform of the third-order polarization,

$$\begin{aligned} I(\omega;\tau,T) &= |E^{(3)}(\omega;\tau,T)|^2 \\ &\propto |P^{(3)}(\omega;\tau,T)|^2 \\ &\propto |\mathrm{Re}\int_0^\infty \mathrm{d}t' \exp(\mathrm{i}\omega t')\, P^{(3)}(\tau;T,t')|^2 \end{aligned} \tag{1}$$

where $P^{(3)}(\tau,T,t')$ is the third-order polarization at time t' with the electric fields of the input pulses subsumed in it. In an experiment employing a delta function (or spectrally uniform) probe pulse, eq 1 directly represents the spectrum of a transient grating at time T. Otherwise, the SRFWM signal needs to be normalized by the probe spectrum to give a transient spectrum at time T:[21]

$$I'(\omega;\tau,T) = \frac{I'(\omega;\tau,T)}{I_{\mathrm{probe}}(\omega)} \tag{2}$$

Response function theory on third-order nonlinear spectroscopies in frequency and time domains has been described in detail in a monograph by Mukamel.[22] The response functions, R_i, leading to the third-order polarization, $P^{(3)}(\tau,T,t')$, can be calculated from an $M(t)$, the transition frequency correlation function:

$$M(t) = \frac{\langle \Delta\omega(t)\, \Delta\omega(0)\rangle}{\langle \Delta\omega^2\rangle} \tag{3}$$

where $\Delta\omega(t) = \langle\omega\rangle - \omega(t)$, $\omega(t)$ is the transition frequency at time t and the brackets denote an ensemble average. The $M(t)$ may include intramolecular as well as intermolecular processes. There are four time evolution pathways (Figure 1a) to create $P^{(3)}(\tau,T,t')$. Formally, the response functions may be divided into the ground state, R_g, and the excited state, R_e, contributions according to a molecular state during the population period T:[6,22]

$$R = R_e + R_g \tag{4a}$$

$$\begin{aligned} R_e &= R_1 + R_2 \\ &= \mathrm{Tr}[G_{eg}(t')\, G_{ee}(T)\, G_{ge}(\tau)\rho_g] + \\ &\qquad \mathrm{Tr}[G_{eg}(t')\, G_{ee}(T)\, G_{eg}(\tau)\rho_g] \end{aligned} \tag{4b}$$

$$\begin{aligned} R_g &= R_3 + R_4 \\ &= \mathrm{Tr}[G_{eg}(t')\, G_{gg}(T)\, G_{ge}(\tau)\rho_g] + \\ &\qquad \mathrm{Tr}[G_{eg}(t')\, G_{gg}(T)\, G_{eg}(\tau)\rho_g] \end{aligned} \tag{4c}$$

Here ρ_g is the thermal density matrix and G is the Liouville space propagator defined as

$$G_{ab}(t)A = \exp(-\mathrm{i}H_a t)A \exp(\mathrm{i}H_b t)$$

where A is an arbitrary operator and H_i is the Hamiltonian in state i. As shown in eqs 4, the system propagates under the ground (R_g) or the excited-state (R_e) Hamiltonian during time T. The R_i's can be calculated by a cumulant expansion as described in detail in the literature.[22]

For a two-level system, SRFWM consists of two contributions: excited-state stimulated emission and ground-state bleach. A pair of pump pulses excites molecules creating a particle in the electronic excited state, while leaving a hole in the ground state. During T, molecules in the excited-state undergo solvation, which is manifested in the dynamic Stokes shift. The hole in the ground state is filled up during T by the fluctuation of the transition frequencies of molecules in the ground state. The hole and the particle dynamics are described by R_g and R_e, respectively. Assuming linear response (harmonic potential curves), the fluctuation−dissipation theorem implies that $M(t)$ for the molecules in the ground state (equilibrium fluctuation) is equivalent to $M(t)$ for the molecules in the excited states (dissipation). When nonlinear response effect becomes significant, the response functions, R_i, must be calculated separately using different $M(t)$'s for the ground and the excited-state pathways. For a system with two electronic levels but with vibronic structures, excitation by pump pulses with their durations shorter than vibrational periods creates vibrational wave packets in both the ground and the excited electronic states. The nuclear wave packets decay by the vibrational dephasing time in the corresponding states. The vibrational wave packets in different electronic states are of course different and must be treated separately. The nuclear wave packet motion can be incorporated into the above formalism by addition of underdamped harmonic oscillators in $M(t)$.[6,22]

Experimentally, the stimulated emission spectrum (R_e) develops on the red side of the 0−0 transition frequency, while the ground-state bleach spectrum (R_g) appears on the blue side. For a molecule with large Stokes shift, they may appear as two separated bands. In this case, the ground-state hole and the excited-state particle dynamics can be observed separately. Quite often, however, a Stokes shift is not large enough for SRFWM to be divided into two separated bands.

To illustrate SRFWM for a realistic system, especially for a system with small Stokes shift, we have calculated the signal according to eq 1 including finite pulse duration. It needs to be emphasized that the ground-state bleach spectrum is not sensitive to the dynamics in $M(t)$ for a delta function pump pulse, since no hole in the absorption spectrum is created for white light (delta function pulse) excitation.[23] Also, vibrational wave packets can only be created using pulses of finite duration.[24] In the calculation we have used an $M(t)$ of DTTCI in methanol

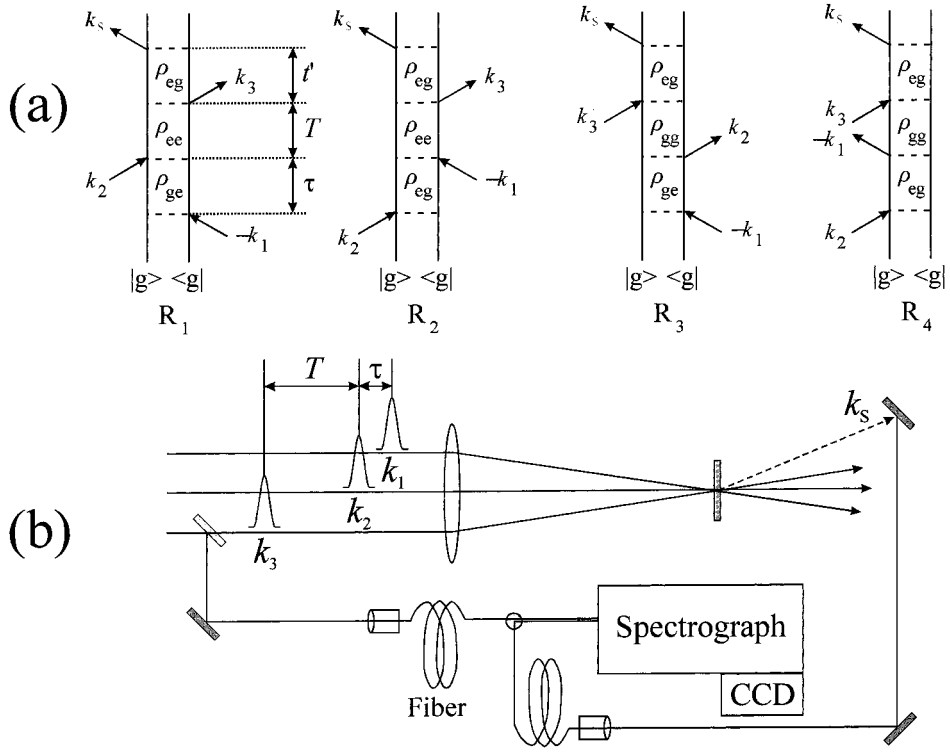

Figure 1. (a) Two-level system (ground, |g⟩, and excited, |e⟩ states) double-sided Feynman diagrams for the third-order polarization into the phase matching direction $-k_1 + k_2 + k_3$. ρ_{ij} are the system density matrix elements, 1−3 denote input pulses, and S denotes the signal. After the second field-matter interaction, populations in the excited state are created by R_1 and R_2 time evolution pathways while the system resides in the ground state for R_3 and R_4. (b) Experimental layout for the SRFWM measurements. Spectra of the signal (k_s) and the probe pulse (k_3) are measured simultaneously by a two-leg fiber. Pulse sequences and notations for time intervals are also indicated.

reported previously.[25] The model $M(t)$ excluding vibrational contribution is

$$M(t) = 0.7\exp(-t/260\text{ fs}) + 0.25\exp(-t/3.3\text{ ps}) + 0.05\exp(-t/9.5\text{ ps}) \quad (5)$$

In addition, two underdamped cosinusoids are included to account for the vibrational wave packets: a 500 cm^{-1} mode is added to eq 5 to form an $M(t)$ in the ground state, which is used to calculated R_g in eq 4c; similarly, a 150 cm^{-1} mode is included for the excited-state pathways. The solvent reorganization energy, λ_s, of 217 cm^{-1} is used in the calculation.[26] Frequencies of the pump pulses are tuned to +217 cm^{-1} from the 0−0 transition frequency, i.e., the center of stationary absorption spectrum. Figure 2a shows SRFWM at several different T values calculated for 18 fs pump pulses and a delta function probe pulse. The ground-state bleach and the stimulated emission spectra at $T = 0$ are all identical, as they should be. In a realistic polyatomic molecule where many vibrational modes are present, stimulated emission shifts initially by an ultrafast <10 fs time scale due to ultrafast rupture of the vibrational wave packets.[6] Stimulated emission is usually regarded to be centered at 0−0 transition frequency even at $T = 0$,[13] because of the limited time resolution in most experiments. In Figure 2a the stimulated emission clearly shifts to the red as T increases, although it is not easy to see the change in the bleach spectra. To show the changes in the spectra more clearly, each of the bleach and the stimulated emission spectrum at a given T is fitted to a single log-normal function to find the center frequency, which is shown in Figure 2b. As T increases, the stimulated emission shifts to the red due to solvation given by eq 5. At the same time, the emission center frequency oscillates by the excited-state vibrational period 222 fs (150 cm^{-1}). The ground-state bleach spectrum oscillates around the absorption center frequency by the ground-state vibrational period 66.7 fs (500 cm^{-1}). Were the pump frequencies tuned to the 0−0, the bleach would start from the 0−0 frequency (−217 cm^{-1}) and shift to the blue as T increases.

Although the center frequencies of the bleach and the stimulated emission spectra are separated by ∼400 cm^{-1} at $T = 2$ ps, the sum (SRFWM) appears as a single peak, as shown in Figure 2a. In an experiment with similar circumstances, it would be unreasonable to resolve the spectra into a ground-state bleach and a stimulated emission to observe the ground- and excited-state dynamics separately. Even in this situation, however, an oscillation in the center frequency of the whole spectra can still be assigned to either the ground or the excited electronic state unambiguously by comparison between the phase of the oscillation in center frequency and that in line width. To illustrate this point, we have fitted each SRFWM spectrum to a single log-normal function to obtain a center frequency and a line width. The center frequencies and the line widths vs T are shown in Figure 3. It can be seen that the phases of the vibration in the ground state (500 cm^{-1}) are in-phase with each other, as indicated by the vertical bar B, while they are out-of-phase for the vibration (150 cm^{-1}) in the excited state (vertical bar A). This can be understood easily as follows: Consider a two-level system in which the excited-state potential surface is a replica of the ground-state potential surface but displaced horizontally by d from that of the ground and vertically displaced by the 0−0 transition frequency. Assuming harmonic potential surfaces, the classical Franck principle says that the electronic transition frequency is proportional to the nuclear coordinate with negative proportionality constant. As the ground-state wave packet moves toward the inner turning point, the bleach spectrum moves to a higher frequency to make the center frequency of SRFWM increase. Meanwhile, the separation of

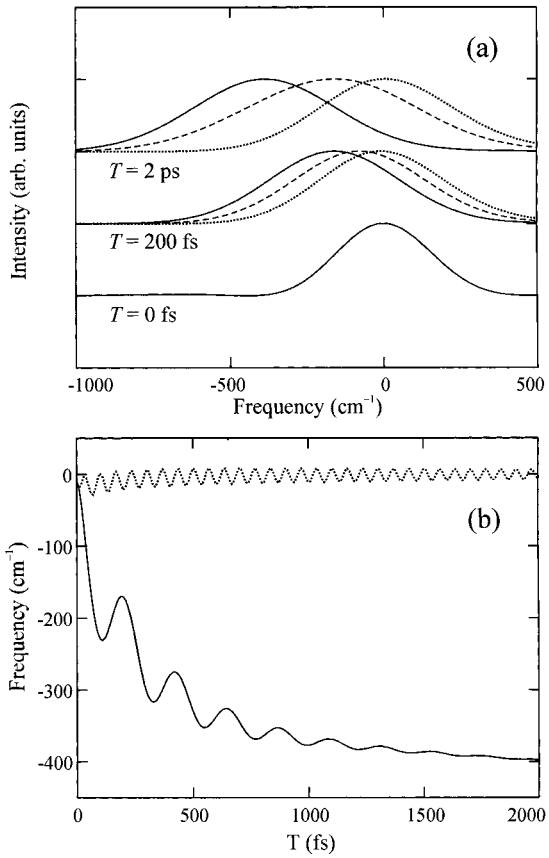

Figure 2. (a) Calculated SRFWM signals using 18 fs pump pulses and a delta function probe pulse. τ is set to zero. Stimulated emission (R_1 and R_2, solid line), ground-state bleach (R_3 and R_4, dotted line), and the sum of the two (R_1-R_4, dashed line) are shown separately. All three overlap at $T = 0$ fs. (b) Center frequency of the ground-state bleach (dotted line) and stimulated emission (solid line) spectra. Nonlinear least-squares fits to a single log-normal function are used. Frequency of the absorption maximum excluding vibronic structure is defined as 0 cm^{-1}.

the bleach and the stimulated emission increases, which causes the SRFWM line width to increase. On the contrary, as the wave packet in the excited-state moves toward the inner turning point, the stimulated emission spectrum approaches toward the bleach spectrum. That is, the center frequency of SRFWM increases, while the line width decreases to make the phases between the two 180° out of phase.

When the ground-state bleach and the stimulated emission cannot be resolved, the sensitivity of the SRFWM center frequency on nuclear wave packet dynamics depends on the frequency and duration of pump pulses as well as the molecular parameters. In particular, when the pump is tuned to the 0−0 transition frequency, and the nuclear wave packets in the ground and in the excited states are equal in frequencies and amplitudes but moving in opposite direction, the center frequency becomes insensitive to the wave packet dynamics. Although this condition can rarely be met in real systems, the sensitivity of the SRFWM center frequency decreases in a 0−0 excitation condition. For a system with a large Stokes shift, the ground-state bleach and the stimulated emission can be resolved as two separate bands. Solvation dynamics, ground-state hole filling, and the wave packet dynamics in each state can be observed separately.

3. Experimental Section

The experimental apparatus has been described in detail elsewhere.[25] The light source is a home-built cavity-dumped

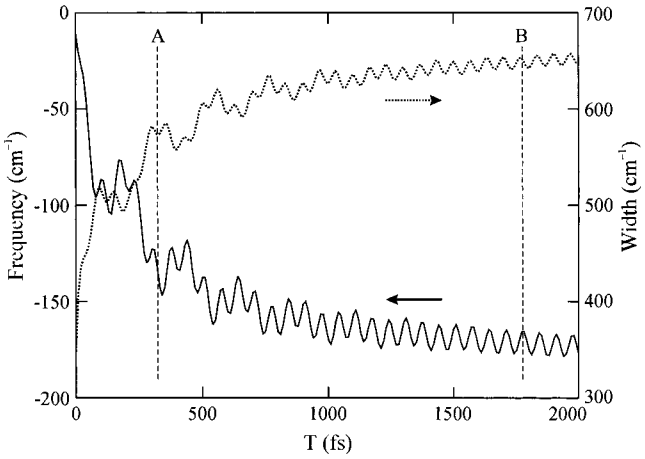

Figure 3. Center frequency (solid line) and the line width (dotted line) of the calculated SRFWM shown in Figure 2a. Nonlinear least-squares fits to a single log-normal function are used.

Kerr lens mode-locked Ti:sapphire laser generating 18 fs pulses centered at 795 nm. The repetition rate and energy of the pulses were adjusted to 150 kHz and 3 nJ, respectively, to avoid any power-induced artifacts including photoisomerization.

The laser output was split into three roughly equal energy pulses and focused in "Box" geometry to a 200 μm thick flow cell containing the sample solution. The third-order nonlinear signal into $-k_1 + k_2 + k_3$ phase matching direction was spatially filtered and directed to a spectrograph equipped with a CCD array detector. Spectra of the third-order nonlinear signal and the probe pulse (k_3) were measured simultaneously by using a two-leg fiber, as shown in Figure 1. We have employed a polarization scheme to reduce noises from scattering of the input beams: k_2 and k_3 are polarized parallel to an optical table, while k_1 is perpendicular to the table. The signal, having perpendicular polarization, was filtered by a polarizer in front of the detector. The background noise was much smaller than the signal even at large T.

A cyanine dye DTTCI was used as received from Exciton Co. The concentration of DTTCI in methanol solution was adjusted to give an absorbance ~0.3 at absorption maximum (758 nm). All the measurements were performed for a freshly prepared solution, since the UV/vis absorption spectra of the dye solution develop a sign of degradation in a few days. A spontaneous fluorescence spectrum of the solution was recorded in a backscattering geometry using the same detection apparatus used above and a He−Ne laser (632.8 nm) as an excitation source. All of the measurements were performed at ambient temperature (22 ± 1°C).

4. Results and Discussion

Spectrum of the femtosecond pulse used is broad enough to cover most of the wavelength region that stationary absorption and emission of DTTCI in methanol appear. Normalization by the probe spectrum according to eq 2 can be applied reliably over the wavelength region 730−860 nm. Representative SRFWM signals for several T values as well as the stationary absorption and spontaneous emission spectra are shown in Figure 4. The SRFWM signals can be well represented by a sum of the stationary emission and the absorption, although the relative contribution of the absorption is about 35% of the stimulated emission. Oscillation of the peak position is readily apparent for small T's, while the spectra seem to shift to the red monotonically for T values from 518 fs to 20 ps. The origins of a small bump at 13 500 cm^{-1} and modulation in the spectra

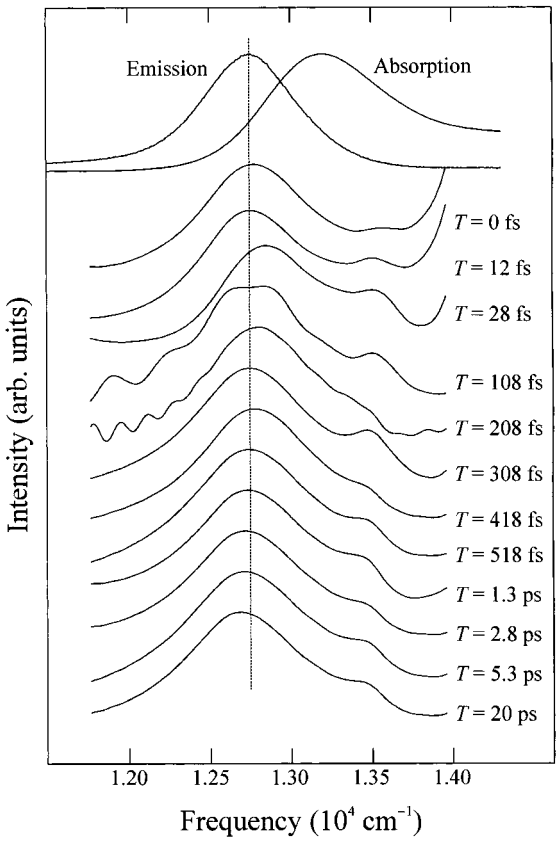

Figure 4. Representative SRFWM signals for several *T* values as well as the stationary absorption and spontaneous emission spectra of DTTCI in methanol.

for $T = 108$, 208 fs are unclear and will not be pursued in this work. Cyanine dyes such as HITCI and DTTCI are known to undergo isomerization in the S_1 state.[27,28] Moreover, the photoisomers of DTTCI and HITCI may absorb near 800 nm. Photoisomerization products, however, are usually observed when the molecules are excited on the blue side of the absorption band with a much higher pulse energy than used here.[17,28] If photoisomerization occurs significantly, one would observe a feature that may be attributable to photoisomerization intermediates and/or photoisomerization products. No such band has been found. However, the fact that the relative contribution of the ground-state absorption to SRFWM is smaller than the stimulated emission still leaves the possibility of photoisomerization products absorbing near the stationary absorption wavelength.

The SRFWM signals shown in Figure 4 appear as a single band, and the separation into the ground-state bleach and the stimulated emission spectra cannot be realized. Instead, we have fitted each spectrum to a single log-normal function. The results are shown in Figure 5, which demonstrates that center frequency and line width can be measured with a precision better than 10 cm^{-1} by SRFWM technique. The shape of the center frequency vs *T* is in general quite similar to the solvation function of methanol reported previously by using various methods.[5,6,13,16,25] The center frequency decreases as *T* increases because of the dynamics Stokes shift of the stimulated emission band. On the other hand, the line width increases as *T* increases mainly because the ground-state bleach and the excited-state stimulated emission band bands are separated more as solvation proceeds. This observation is in contrast to a report by Bingemann and Ernsting[16] where an initial rapid decrease of the line width on a 100 fs time scale followed by a subsequent increase on picosecond time scales has been observed. The behavior of the

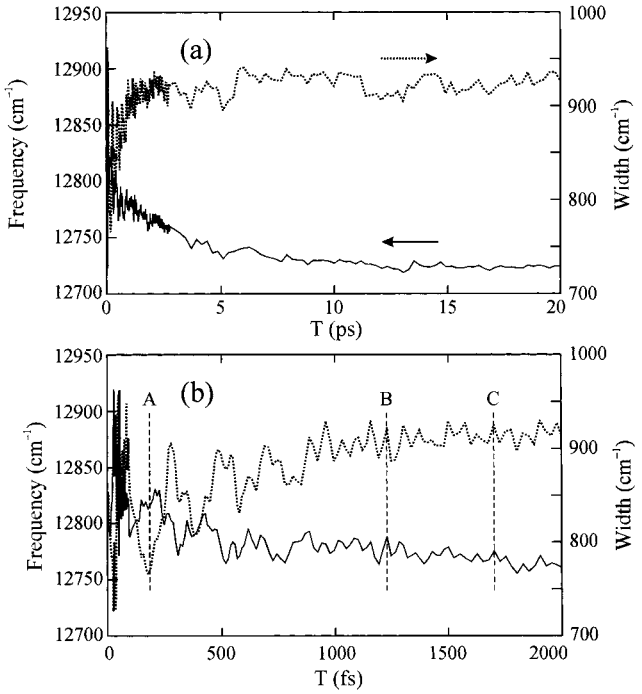

Figure 5. Center frequency (solid line) and the line width (dotted line) of the SRFWM of DTTCI in methanol shown in two different time scales.

center frequency and the line width observed in this work is in good agreement with the model calculations in section 2.

Solvation dynamics of DTTCI in methanol has been reported previously by using three pulse-stimulated photon echo peak shifts (3PEPS).[5,25] The $M(t)$ reported excluding intramolecular vibrations was shown in eq 5. In this work, the center frequency (in units of cm^{-1}) is well described by 2 exponentials in a nonlinear least-squares fit:

$$\omega_c(t) = 49\exp(-t/235\text{ fs}) + 70\exp(-t/4.2\text{ ps}) + 12722 \quad (6)$$

The time constants are in good agreement with previous results, although the 4.2 ps component cannot be resolved into two picosecond components as in a previous report.[25] The relative amplitude of the 235 fs component is smaller than the values reported previously. We believe the small ultrafast component is caused by the detuning of the pump laser frequencies from absorption maximum. When the excitation frequency is tuned on the red side of the absorption maximum, the ground-state bleach spectrum shifts toward the stationary absorption spectrum, a blue shift, as *T* increases. The red shift of the stimulated emission due to solvation is partially canceled by the blue shift of the bleach band, the degree of cancellation determined by the exact position of the excitation frequency. The solvation dynamics of a dye molecule in methanol has been much discussed in the literature and will not be discussed any further. We simply point out the sluggishness of the initial solvation for DTTCI in methanol compared to a typical value of 100 fs using other dyes as probe molecules.[6,13,29,30]

Also prominent in Figure 5 are the oscillations of the center frequency and the line width. A small amplitude ($\sim$10 cm^{-1}) oscillation at *T* around 2 ps is readily visible demonstrating the precision of the measurements. As shown in section 2, nuclear wave packet motions in both the ground and the excited states are manifested in the oscillation of the center frequency and the line width. To verify that the oscillations are due to

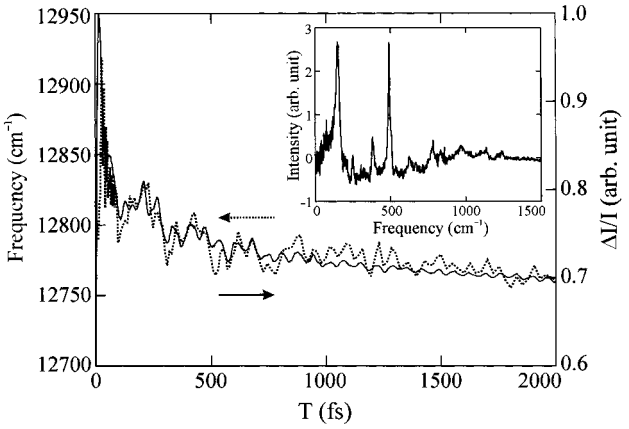

Figure 6. Comparison of the center frequency of SRFWM shown in Figure 5 (dotted line) and the TA (solid line). The inset shows real Fourier transform of the TA.

TABLE 1: Oscillation Components Obtained from the Nonlinear Least Square Fits of the SRFWM Center Frequency and Line Width

		phase (rad)		
frequency (cm^{-1})	time const (fs)	center	width	TA[a]
154	350	−0.085	−2.2	−0.54
379	590	−0.13	−0.82	0.35
492	1200	−1.0	−0.81	−0.2

[a] Obtained by linear prediction singular value decomposition method.

intramolecular vibrations as in TA, we have measured a TA of DTTCI in methanol and compared with the center frequency, which is shown in Figure 6. The Fourier transform of the oscillation components in TA is also shown in Figure 6 as an inset, which shows three prominent vibrations at 154, 379, and 492 cm^{-1}. The Fourier transform of the center frequency and the line width vs T is also similar to the Figure 6 inset.

One important issue in TA spectroscopy is that there exists an ambiguity in the origin of an oscillation (vibration) to either one of the two electronic states involved.[9,31] This may have an important consequence in the interpretation TA signal related with chemical reaction dynamics.[32] On the basis of the following observations, we argue that the 154 and 492 cm^{-1} modes in the center frequency of the SRFWM are due to the vibrational wave packet motions in the excited and the ground electronic states, respectively, at least for the present experimental conditions. It has been shown in section 2 that the center frequency and the line width vs T in an SRFWM move in phase for a wave packet motion in the ground state, while they move out of phase in the excited state. It can be seen clearly in Figure 5 that the center frequency and the line width have the same phase for the 492 cm^{-1} mode (see vertical bars B and C in Figure 5b). On the contrary, for the 154 cm^{-1} mode the phase in the line width is roughly 180° out-of-phase from that in the center frequency (see vertical bar A). To support visual inspection, we have nonlinear least-squares fitted the center frequency and the line width to retrieve oscillation frequencies, decay times, and the phases. The corresponding values from TA data are extracted by linear prediction singular value decomposition method.[33] The fit results are listed in Table 1. The phases from TA are all close to zero in agreement with theoretical considerations.[23] The phases in the center frequency and line width for the 492 cm^{-1} mode are about the same, while they are roughly out-of-phase for the 154 cm^{-1} mode. The dephasing time of the 154 cm^{-1} mode is also relatively short, 350 fs, to justify the assignment.

5. Concluding Comments

We have shown that frequency−time-resolved spectrogram can be obtained easily by spectrally resolving a background-free three pulse four-wave mixing signal in a transient grating (TG) geometry. Although the information that can be obtained from SRFWM is the same as that from dispersed pump/probe TA in the current experimental condition, the background-free geometry allows sensitive spectra measurements employing array detectors.

In general, TG and TA signals are not equivalent. Transient grating consists of the intensity grating and the refractive index grating. When the time delay of the two pump pulses (τ in eq 1) is not zero, a transient grating in frequency space is also present. Consequently, TG signal intensity is sensitive on spatial and spectral diffusion processes. Once their signals are spectrally dispersed, the TG and TA spectra are much more alike (except the frequency grating in TG), since the spatial diffusion processes unique to TG becomes irrelevant. However, SRFWM and dispersed TA are different in one important aspect. In the presence of excited-state absorption, dispersed TA can have negative values, but SRFWM is always positive due to the detection of the modulus squared of the polarization.

By utilizing SRFWM and theoretical calculations, we have studied the solvation dynamics and the nuclear wave packet motions in the ground and the excited states for a dye molecule in methanol solution with sub 20 fs time resolution. The spectra are well described as a sum of the time-dependent ground-state bleach and the excited-state stimulated emission spectra. Although the spectra cannot be divided into bleach and stimulated emission contributions due to a small Stoke shift, the center frequency and the line width carry detailed information on the solvation dynamics and nuclear wave packet motions. In addition to the frequency shifts due to solvation process, the center frequency and the line width show oscillations due to the nuclear wave packet motions in both the ground and the excited electronic states. The ambiguity in assignment of an oscillation to either the ground or the excited electronic states can be resolved by comparison between the phase in the line width and that in the center frequency for the oscillation.

Acknowledgment. Financial support was provided by the Korea Science and Engineering Foundation (96-0501-02-01-3) and in part by CRM-KOSEF (1999).

References and Notes

(1) See for example: *Ultrafast Phenomena X*; Barbara, P. F., Fujimoto, J. G., Knox, W. H., Zinth, W., Eds.; Springer: Berlin, 1996; Part VII.

(2) (a) Stanley, R. J.; Boxer, S. G. *J. Phys. Chem.* **1995**, *99*, 859. (b) Stanley, R. J.; King, B.; Boxer, S. G. *J. Phys. Chem.* **1996**, *100*, 12052.

(3) Rubtsov, I. V.; Yoshihara, K. *J. Phys. Chem. A* **1997**, *101*, 6138.

(4) Joo, T.; Jia, Y.; Yu, J.-Y.; Jonas, D. M.; Fleming, G. R. *J. Phys. Chem.* **1996**, *100*, 2399.

(5) de Boeij, W. P.; Pshenichnikov, M. S.; Wiersma, D. A. *J. Phys. Chem.* **1996**, *100*, 11806.

(6) Joo, T.; Jia, Y.; Yu, J.-Y.; Lang, M. J.; Fleming, G. R. *J. Chem. Phys.* **1996**, *104*, 6089.

(7) Heller, E. J. *Acc. Chem. Res.* **1981**, *14*, 368.

(8) Scherer, N. F.; Jonas, D. M.; Fleming, G. R. *J. Chem. Phys.* **1993**, *99*, 153.

(9) Bardeen, C. J.; Wang, Q.; Shank, C. V. *J. Phys. Chem. A* **1998**, *102*, 2759.

(10) Kahlow, M. A.; Jarzeba, W.; DuBruil, T. P.; Barbara, P. F. *Rev. Sci. Instrum.* **1988**, *59*, 1098.

(11) Castner, E. W.; Maroncelli, M.; Fleming, G. R. *J. Chem. Phys.* **1987**, *86*, 1090.

(12) Barbara, P. F.; Jarzeba, W. *Adv. Photochem.* **1990**, *15*, 1.

(13) Horng, M. L.; Gardecki, J. A.; Papazyan, A.; Maroncelli, M. *J. Phys. Chem.* **1995**, *99*, 17311.

(14) Rosenthal, S. J.; Xie, X. L.; Du, M.; Fleming, G. R. *J. Chem. Phys.* **1991**, *95*, 4715.

(15) Brito Cruz, C. H.; Fork, R. L.; Knox, W. H.; Shank, C. V. *Chem. Phys. Lett.* **1986**, *132*, 341.

(16) Bingemann, D.; Ernsting, N. P. *J. Chem. Phys.* **1995**, *102*, 2691.

(17) Kovalenko, S. A.; Ernsting, N. P.; Ruthmann, J. *J. Chem. Phys.* **1997**, *106*, 3504.

(18) Ruthmann, J.; Kovalenko, S. A.; Ernsting, N. P.; Ouw, D. *J. Chem. Phys.* **1998**, *109*, 5466.

(19) Book, L. D.; Scherer, N. F. *J. Chem. Phys.* **1999**, *111*, 792.

(20) Brown, E. J.; Pastirk, I.; Grimberg, B. I.; Lozovoy, V. V.; Dantus, M. *J. Chem. Phys.* **1999**, *111*, 3779.

(21) The equation is exact when the pump and the probe pulse are well separated in time and the probe pulse duration is short enough such that nuclear dynamics is negligible over the pulse duration.

(22) Mukamel, S. *Principles of Nonlinear Optical Spectroscopy*; Oxford: New York, 1995.

(23) Jonas, D. M.; Bradforth, S. E.; Passino, S. A.; Fleming, G. R. *J. Phys. Chem.* **1995**, *99*, 2594.

(24) Bosma, W. B.; Yan, Y. J.; Mukamel, S. *J. Chem. Phys.* **1990**, *93*, 3863.

(25) Lee, S.-H.; Lee, J.-H.; Joo, T. *J. Chem. Phys.* **1999**, *104*, 6089.

(26) The Stokes shift due to solvation is $2\lambda_s$. The corresponding coupling strength Δ ($=\langle\Delta\omega^2\rangle^{1/2}$) in the high-temperature limit is 300 cm^{-1}. In the absence of vibronic structures, the stationary absorption maximum is at $\omega_{00} + \lambda_s$ and the fluorescence maximum in the long time limit is at $\omega_{00} - \lambda_s$, where ω_{00} is the 0−0 transition frequency.

(27) Fouassier, J.-P.; Lougnot, D.-J.; Faure, J. *Chem. Phys. Lett.* **1975**, *35*, 189.

(28) Kobayashi, T.; Nagakura, S. *Chem. Phys.* **1977**, *23*, 153.

(29) Shirota, H.; Pal, H.; Tominaga, K.; Yoshihara, K. *J. Phys. Chem.* **1996**, *100*, 14575.

(30) Gustavsson, T.; Cassara, L.; Gulbinas, V.; Gurzadyan, G.; Mialocq, J.-C.; Pommeret, S.; Sorgius, M.; van der Meulen, P. *J. Phys. Chem.* **1998**, *102*, 4229.

(31) Joo, T.; Albrecht, A. C. *Chem. Phys.* **1993**, *173*, 17.

(32) Wang, Q.; Schoenlein, R. W.; Peteanu, L. A.; Mathies, R. A.; Shank, C. V. *Science* **1994**, *266*, 422.

(33) Barkhuijsen, H.; de Beer, R.; Bovée, W. M. M. J.; van Ormondt, D. *J. Magn. Reson.* **1985**, *61*, 465.